

Lethality rescue and long-term amelioration of a citrullinemia type I mouse model by neonatal gene-targeting combined to SaCRISPR-Cas9

Michela Lisjak,¹ Alessandra Iaconcig,¹ Corrado Guarnaccia,¹ Antonio Vicidomini,¹ Laura Moretti,¹ Fanny Collaud,^{2,3} Giuseppe Ronzitti,^{2,3} Lorena Zentilin,¹ and Andrés F. Muro¹

¹International Centre for Genetic Engineering and Biotechnology, 34149 Trieste, Italy; ²Généthon, 91000 Évry, France; ³Université Paris-Saclay, Université d'Évry, Inserm, Généthon, Integrare Research Unit UMR_S951, 91000 Évry, France

Citrullinemia type I is a rare autosomal-recessive disorder caused by deficiency of argininosuccinate synthetase (ASS1). The clinical presentation includes the acute neonatal form, characterized by ammonia and citrulline accumulation in blood, which may lead to encephalopathy, coma, and death, and the milder late-onset form. Current treatments are unsatisfactory, and the only curative treatment is liver transplantation. We permanently modified the hepatocyte genome in lethal citrullinemia mice (*Ass1*^{fold/fold}) by inserting the *ASS1* cDNA into the albumin locus through the delivery of two AAV8 vectors carrying the donor DNA and the CRISPR-Cas9 platform. The neonatal treatment completely rescued mortality ensuring survival up to 5 months of age, with plasma citrulline levels significantly decreased, while plasma ammonia levels remained unchanged. In contrast, neonatal treatment with a liver-directed non-integrative AAV8-AAT-h*ASS1* vector failed to improve disease parameters. To model late-onset citrullinemia, we dosed postnatal day (P) 30 juvenile animals using the integrative approach, resulting in lifespan improvement and a minor reduction in disease markers. Conversely, treatment with the non-integrative vector completely rescued mortality, reducing plasma ammonia and citrulline to wild-type values. In summary, the integrative approach in neonates is effective, although further improvements are required to fully correct the phenotype. Non-integrative gene therapy application to juvenile mice ensures a stable and very efficient therapeutic effect.

INTRODUCTION

Citrullinemia type I (CTLNI; Online Mendelian Inheritance in Man [OMIM] 215700) is an autosomal-recessive inherited disorder caused by the deficiency of argininosuccinate synthetase (ASS1). ASS1, the third enzyme of the urea cycle, is involved in the condensation of citrulline and aspartate into argininosuccinate.¹ Mutations in the *ASS1* gene lead to a pathological alteration of the urea cycle causing increased blood ammonia levels. CTLNI presents as a spectrum that includes a neonatal acute form (the “classic” form) and a milder late-onset form (the “non-classic” form).² The acute neonatal form

presents right after birth with acute hyperammonemia and life-threatening encephalopathy, which can lead to early death if not immediately treated. Infants who survive a severe episode of neonatal hyperammonemia often experience complications, such as unrecoverable neurological damage and developmental delays. Late-onset patients present milder phenotypes, including delayed mental and physical development, neurodisability, somnolence, and chronic intermittent hyperammonemia during childhood and adulthood. The estimation of prevalence in the population of the severe neonatal form is 1 in 44,300–200,000 depending on population consanguinity.²

The palliative treatment for maintaining low ammonia levels consists in the restriction of protein intake, together with ammonia scavengers and arginine supplementation,³ while liver transplantation is the only established curative treatment, with all the limitations of the approach.^{4,5} Even if liver transplantation became a very effective curative treatment for CTLNI, it is a very invasive procedure with several limitations.

Therefore, there is a clinical need to develop non-invasive alternative treatments to prevent short- and long-term CTLNI complications. Liver-specific adeno-associated virus (AAV)-mediated gene replacement therapy represents a promising alternative option. It has shown safety and long-term efficacy in pre-clinical studies with animal models and clinical trials of adult patients.^{6–13} This strategy is currently being tested in clinical trials in adult patients suffering from late-onset ornithine transcarbamylase (OTC), another urea cycle disease, by Ultragenyx Pharmaceutical (ClinicalTrials.gov identifier NCT05345171). However, in neonatal settings, this approach presents important limitations. In the growing liver the viral episomal DNA may be lost associated with hepatocyte proliferation, decreasing the therapeutic efficiency.^{14–16} Previous studies on citrullinemia with

Received 8 May 2023; accepted 25 August 2023;
<https://doi.org/10.1016/j.omtm.2023.08.022>

Correspondence: Andrés F. Muro, International Centre for Genetic Engineering and Biotechnology (ICGEB), Padriciano 99, 34149 Trieste, Italy.
E-mail: andres.muro@icgeb.org



an AAV-mediated gene replacement therapy have failed to rescue neonatal lethality after a single AAV administration at birth in an *Ass1* knockout (KO) mouse model.^{17,18} Successful lethality rescue was achieved only after the intra-uterine administration of the therapeutic AAV vector followed by multiple AAV re-administrations after birth.¹⁷ Although this strategy was successful in neonate *Ass1* KO mice, gene therapy efficacy after repeated administration in human patients may be hampered by the generation of anti-AAV neutralizing antibodies,^{8,19} posing an important limit to this approach. Genome editing and gene targeting strategies are promising alternatives to overcome the loss of the episomal therapeutic DNA as they permanently modify the hepatocyte genome, resulting in the transmission of the genetic modification to daughter cells and assuring long-term correction.^{20,21}

Here, we compared the AAV-mediated gene-replacement episomal approach with a dual AAV CRISPR-Cas9-mediated genome targeting strategy, at two disease-relevant ages: postnatal day (P) 2, representing the early onset, more severe CTLNI condition, and juvenile P30, representing late-onset CTLNI patients. The episomal gene therapy approach involves AAV-mediated delivery of a cDNA encoding for the human *ASS1* enzyme under the control of a liver-specific promoter.²² The genome targeting strategy, also called GeneRide,^{23,24} is based on the insertion of a promoterless human *ASS1* cDNA into the 3' coding region of the albumin (*Alb*) gene, with the use of engineered nucleases to increase targeting rate.^{25,26} After recombination, the targeted transgene remains under the transcriptional control of the strong albumin promoter.²⁷

We have shown that both approaches were able to rescue the lethal phenotype and the main disease markers of CTLNI mice. In fact, the non-integrative gene therapy approach showed to be very effective in ameliorating the symptoms of the disease in juvenile mice but not in neonate animals. On the other hand, the integrative approach proved to be very efficient in treating mice at the neonatal stage, but the episomal, non-integrative strategy failed to rescue disease markers. Thus, our results indicate that the neonatal-onset form of CTLNI could be efficiently treated with the gene-targeting integrative strategy, while non-integrative AAV-mediated liver gene replacement therapy could be successfully applied for the efficient treatment of late-onset patients.

RESULTS

Generation of human *ASS1* codon-optimized cDNA variants

To find an effective and permanent therapy for CTLNI, we tested our strategy in *Ass1*^{fold/fold} mice, a mouse model for CTLNI.²⁸ First, we generated homozygous mice to verify that the main features of the strain were also reproduced in our hands. We observed that all homozygous mutant mice survived much longer than previously reported.²⁸ In fact, all mice died by P160 when fed with a diet with 18% protein content, with 50% mortality observed at ~90 days (Figure S1A), instead of 21 days, as reported by Perez et al.²⁸ Unfortunately, the protein content present in the diet was not indicated.²⁸ As expected, plasma ammonia and citrulline levels were significantly

increased compared with wild-type (WT) mice (Figures S1B and S1C), although they were lower than those reported by others.^{28,29} *Ass1* protein levels were similar to those of WT animals, although they presented higher individual variability (Figures S1D and S1E).

Aiming at increasing the efficacy of the treatment, we generated four codon-optimized human *ASS1* cDNA variants using different optimization algorithms. These variants were cloned into the pSMD2 vector,²² and tested by transient transfection in HUH-7 liver-derived cells followed by western blot analysis of the *ASS1* protein (Figure S2). We observed about a 3-fold increase in the levels of *ASS1* produced by the variant *ASS1* CO1 cDNA, compared with the plasmid encoding the WT *ASS1* cDNA (Figures S2B and S2C). Thus, we performed the first set of experiments with the WT and CO1 versions of the *ASS1* cDNA.

Comparison of integrative and non-integrative strategies in neonatal *Ass1*^{fold/fold} mice

To determine the best therapeutic strategy at two relevant disease ages (neonatal and juvenile), we prepared two different constructs and relative AAV vector stocks: the rAAV8-a1AAT-h*ASS1* and the rAAV8-Alb-donor-h*ASS1*, for episomal and integrative approaches, respectively (Figure 1). We treated mice at P2, an age that recapitulated the neonatal, severe CTLNI condition, while mutant mice treated at P30 modeled the late-onset form of the disease. To test the non-integrative episomal approach, we used the rAAV8-a1AAT-h*ASS1* vector that contains the WT or CO1 cDNA variants of the *ASS1* cDNA under the transcriptional control of the alpha1 anti-trypsin promoter and apolipoprotein E enhancer (Figure 1A).²² For the integrative approach, we used a donor vector in which the WT or CO1 variant of the *ASS1* cDNA were inserted just upstream of the natural albumin stop codon, in frame with the albumin coding sequence. A 2A peptide coding sequence was placed upstream of the *ASS1* cDNA, right downstream of the albumin coding sequence (Figure 1B).^{27,30} The chimeric mRNA is translated into two separate proteins, albumin, containing a few extra amino acids from the 2A peptide at its C terminus, and *ASS1*, containing a proline at its N terminus.³¹ The CRISPR/SaCas9 platform was used to increase the recombination rate of the donor vector into the albumin locus.²⁶ The AAV8-SaCas9-sgRNA8 vector was co-administered together with the donor vector, carrying the WT or CO1 cDNA variant of the *ASS1* cDNA. The AAV8-SaCas9-sgRNA8 vector encodes for the SaCas9 nuclease and the sgRNA, which target a PAM site present in the downstream albumin intron 14 (donor vector; Figure 1B). To avoid targeting the donor vector, the PAM site was removed from the donor construct.

We then performed a short-term experiment to evaluate the efficacy of the treatments, in which P2 newborn *Ass1*^{fold/fold} mice were dosed with the integrative and non-integrative vectors at P2 and sacrificed at P30 (Figure 2A). We observed a significant decrease in plasma citrulline levels after the treatment with the integrative approach, while the non-integrative episomal approach resulted in a minor

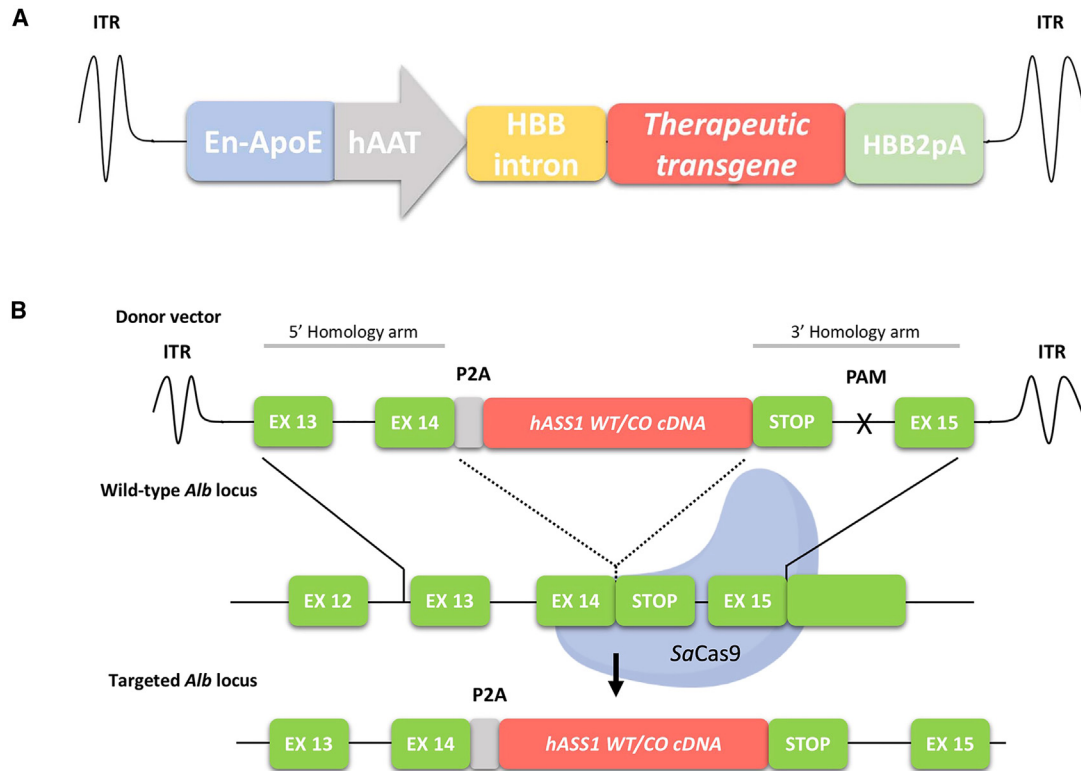


Figure 1. Schemes of the therapeutic strategies

(A) The *hASS1* cDNA codon optimized variants were cloned into the episomal pSMD2 vector containing the strong liver-specific promoter α 1AAT and ApoE enhancer.²² (B) *hASS1* cDNA variants were cloned into a modified version of the donor pAB288 vector containing arms of homology for the albumin locus with the PAM site mutated. After gene targeting, the albumin coding sequence will be followed by a peptide 2A and the therapeutic transgene: *ASS1* WT or codon-optimized.

and statistically nonsignificant reduction of the disease marker (Figure 2B). No variations were observed in the ammonia plasma levels (Figure 2C). Despite the *in vitro* results shown in Figure S2, in both the integrative and episomal approaches, the treatment with the WT *hASS1* cDNA appeared more efficacious than with the CO1 cDNA version. We further analyzed the viral genome copies using genomic PCR to determine potential differences in viral transduction. No statistically significant differences were observed between the values obtained in the mice treated with the integrative approach (Figures S3A and S3B), while a significant difference was observed between the groups treated with the episomal vectors (Figure S3C; $p = 0.02$, *t* test). We also analyzed the levels of transcribed chimeric mRNA levels using qRT-PCR in the livers of mice treated with the integrative strategy. Both groups showed no statistically significant differences, although the group treated with the WT cDNA version presented a trend toward higher levels, compared with the group treated with the CO1 *hASS1* cDNA (Figure S3C). Importantly, no differences were observed in the efficiency of the primers used to amplify the WT and CO1 cDNAs (Figure S3D). Despite having similar mRNA levels, the animals treated with the rAAV8-Alb-donor-CO1-*hASS1* did not present a major improvement in the phenotype compared with those mice treated with the WT

construct. Thus, the next sets of experiments were performed using the WT *hASS1* cDNA.

Long-term correction is obtained with the integrative approach in neonatal *Ass1*^{fold/fold} mice

To determine the appropriate AAV donor dose for the integrative approach, we performed a long-term experiment treating mice with increasing AAV8-donor-WT-*hASS1* vector dosages (2.0E11 vg/pup, 1.0E12 vg/pup, and 2.5E12 vg/pup of AAV8-donor-WT-*hASS1*; and 2.0E11 vg/pup of AAV8-*SaCas9* vector; Figure 3A). All treated mice survived until the end of the experiment, reaching 5 months of age, except for a single animal that died at 140 days (Figure 3B). The mouse that died was treated with the highest dose, presented lowered plasma citrulline levels, and the cause of death was probably not related to the treatment. Weight curves showed a dose-response trend, whereby the group treated with the highest dose reached the most relevant therapeutic effect (Figure 3C). Plasma citrulline levels were significantly lower than those of untreated mutant mice, although not reaching WT levels (Figure 3D). Treated groups presented a dose-dependent reduction in plasma ammonia levels, without reaching WT values, in line with the pattern observed in body weight and plasma citrulline levels (Figure 3E).

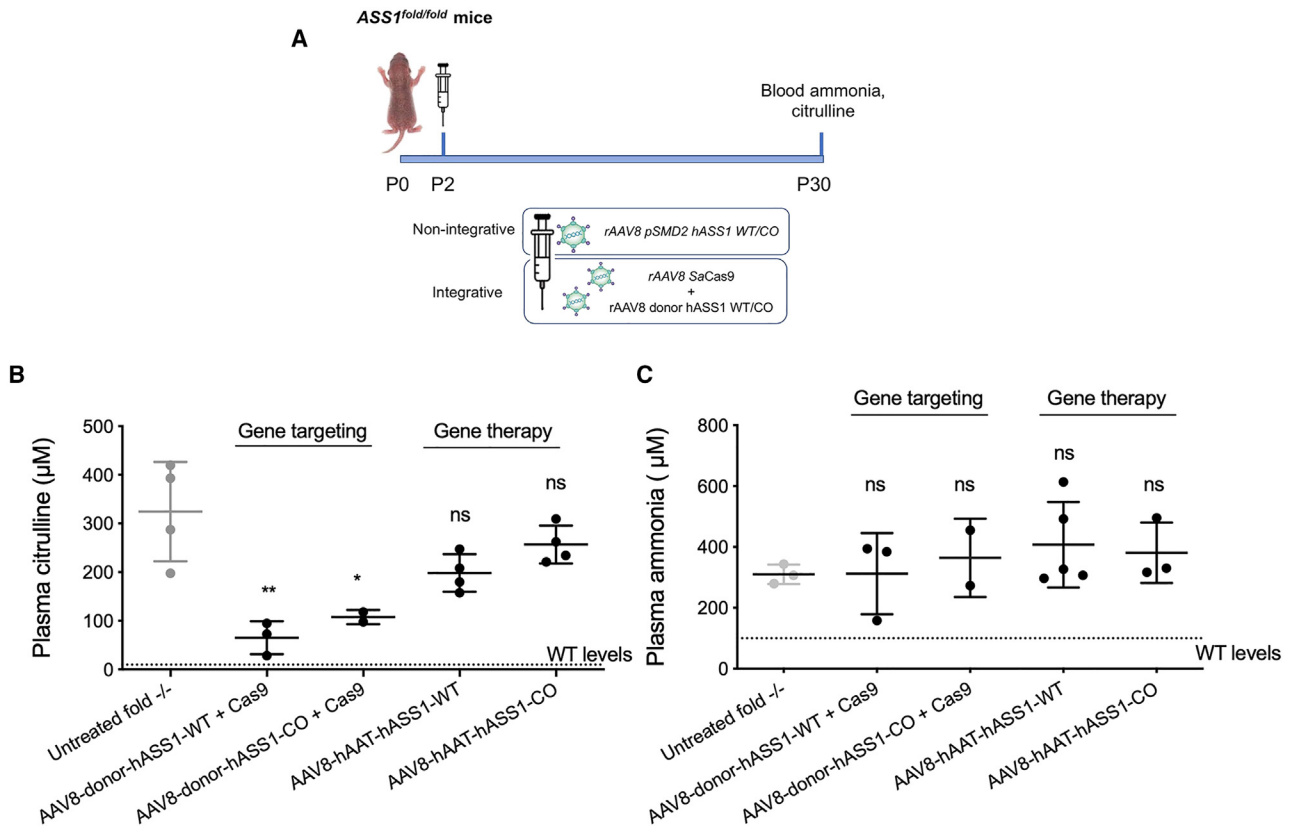


Figure 2. Short-term neonatal study

(A) Scheme of the experimental design: treatment of four groups of *Ass1^{fold/fold}* newborn mice with rAAV8-donor-hASS1 WT (n = 4) or CO (n = 3) (2.0E11 vg/pup) together with rAAV8-SaCas9 (2.0E11 vg/pup) or with the episomal rAAV8-pSMD2-hAAT-hASS1 WT (n = 5) or CO (n = 4) (2.0E11 vg/pup). Mice were sacrificed at 35 days. (B) Plasma citrulline levels were analyzed at P35. Untreated *Ass1^{fold/fold}* mice were used as the control group. Data are shown as mean ± SD and were statistically analyzed using one-way ANOVA with Tukey's multiple-comparisons test (*p < 0.05 and **p < 0.01). (C) Plasma ammonia levels were analyzed at P35. Untreated *Ass1^{fold/fold}* mice were used as the control group. A grid line represents ammonia levels in healthy wild-type mice. Data are shown as mean ± SD and were statistically analyzed using one-way ANOVA with Tukey's multiple-comparisons test (ns, p > 0.05).

Episomal gene therapy is more efficient than the integrative approach in juvenile *Ass1^{fold/fold}* mice

Juvenile, one-month-old *Ass1^{fold/fold}* mice were used to mimic the late-onset form of the disease. Mice were treated with the non-integrative (episomal) and integrative approaches. As we have reported that the rate of homology-directed repair (HDR) could be increased by the simultaneous treatment with fludarabine,³² we also tested the integrative approach by co-treating mutant mice with the HDR enhancer drug, both in the presence or absence of nucleases (Figure 4A). The treatment with the donor construct only (no nucleases/no fludarabine) led to the same mortality that was observed in the untreated group (Figure 4B). Mice treated with the integrative approach with SaCas9, and fludarabine together with the SaCas9, had improved survival, with a survival rate of 75%. The best outcome was observed with the non-integrative, episomal vector (6.0E13 vg/kg rAAV8-AAT-hASS1 WT) and with the integrative approach using fludarabine as HDR enhancer, where all mice survived. In the cohort treated with the episomal vector, the body weight was similar to that

of the untreated WT control mice. In contrast, mice treated with “donor vector alone,” “donor vector with fludarabine,” and “donor plus Cas plus fludarabine” integrative approach displayed a slight increase in body weight compared with the untreated *Ass1^{fold/fold}* group (Figure 4C). However, in the groups treated with the integrative approach, the increment in body size was far from reaching the weight of the WT control group. Western blot analysis showed a statistically significant increase in ASS1 levels in the group treated with the episomal vector, while no evident increase was observed in the groups treated with the integrative approach (Figure S4D). FISH analysis on liver sections of the group treated with the episomal vector revealed that about 16.8% of hepatocytes were positive for the presence of the human *ASS1* mRNA (Figure S4E). Plasma citrulline and ammonia levels of the group treated with the episomal vector were significantly lower than untreated mice, reaching values similar to those of WT control animals. The plasma citrulline and ammonia levels of all other groups were similar to those of untreated mutant mice (Figures 4D and 4E).

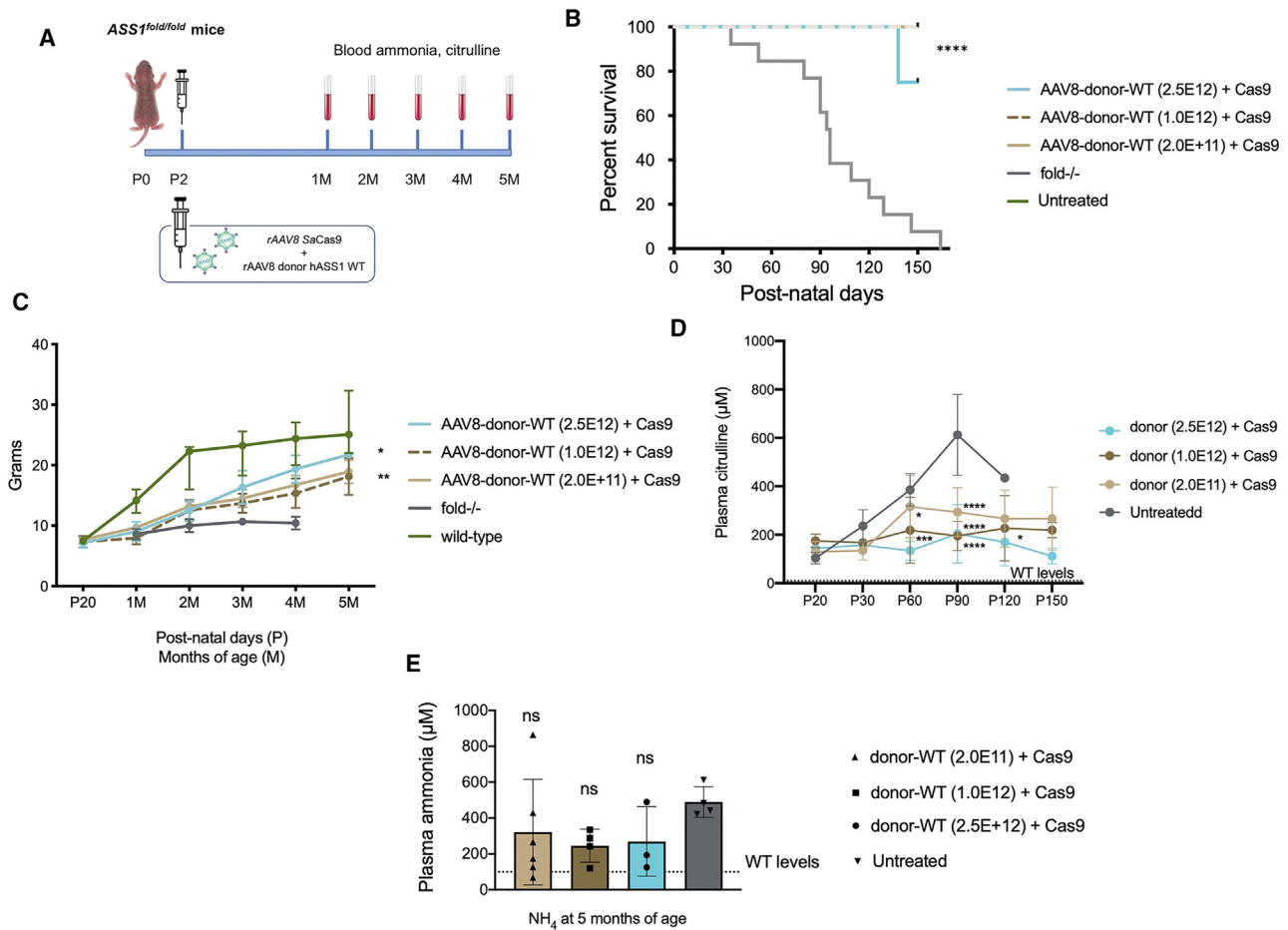


Figure 3. Treatment of neonate *Ass1*^{fold/fold} mice with gene targeting

(A) Scheme of experimental plan. Mice were injected at P2 with AAV-SaCas9 (2.0E11 vg/pup) and with different doses of AAV-donor-hASS1 WT. Blood withdrawal was performed at P20, P30, P60, P90, and P120, and the experiment was terminated at 5 months of age (P150). (B) Kaplan-Meier survival curve. In the curve are represented mice treated with different AAV-donor-hASS1 WT doses together with the AAV-Cas9 and untreated *Ass1*^{fold/fold} animals. All untreated *Ass1*^{fold/fold} mice died before reaching 160 days. Data were analyzed using log-rank test (Mantel-Cox; **** $p < 0.0001$). (C) Growth curve. Body weight mean \pm SD of the three treated groups (2.0E11 vg/pup, $n = 6$; 1.0E12 vg/pup, $n = 4$; 2.5E12 vg/pup, $n = 4$), untreated wild-type ($n = 8$) and *Ass1*^{fold/fold} ($n = 4$) mice are shown. Two-way ANOVA: time, *** $p < 0.001$; treatment, *** $p < 0.001$; interaction, ns. Tukey's multiple-comparisons tests: AAV8-donor-WT (2.5E12) + Cas9 vs. untreated fold-/-, $p = 0.046$; AAV8-donor-WT (2.0E+11) + Cas9 vs. untreated fold-/-, $p = 0.0019$. (D) Plasma citrulline levels. In the graph are represented the plasma citrulline levels of mice treated with different AAV-donor-hASS1 WT vector doses and untreated *Ass1*^{fold/fold} group. Two-way ANOVA: treatment, ** $p < 0.01$; time, *** $p < 0.001$; interaction, *** $p < 0.001$. (E) Plasma ammonia levels. Plasma ammonia levels were determined at 5 months of age in animals with gene targeting treatment. For the untreated *Ass1*^{fold/fold} control group, mice from 2 to 4 months of age were used. Data are shown as mean \pm SD and were statistically analyzed using one-way ANOVA with Tukey's multiple-comparisons test (ns, $p > 0.05$).

To have a deeper insight into the reasons behind the difference in the therapeutic efficacy between neonatal and juvenile-treated mice, we evaluated the recombination rate of the donor vector by digital droplet PCR (ddPCR) of liver genomic DNA. The gene-targeting rate reached 15% in the neonatal mice treated with the higher AAV-donor dose (Figure 5A; Figure S5), while in the juvenile-treated mice the targeting rate reached only 3% in mice treated with only donor vector or donor vector and fludarabine (Figure 5B). The gene-targeting rate was also evaluated using fluorescence *in situ* hybridization (FISH) on liver sections of mice treated at P2, indicating that 9.3% of the hepatocytes expressed the *ASS1* mRNA (Figure 5C). To note, the signal was present in clusters, suggesting that the integra-

tion event occurred soon after vector transduction and the modification was stably transmitted to daughter cells.

DISCUSSION

The only effective therapy available for babies suffering from the classical neonatal-onset form of CTLN1 I, in which residual *ASS1* enzymatic activity is less than 1% of that present in healthy individuals, is orthotopic liver transplantation.^{4,5} Thus, the development of more effective therapies for CTLN1 is a clinical need.

In this study we developed effective AAV-mediated integrative and non-integrative gene therapies for two disease-relevant ages using a

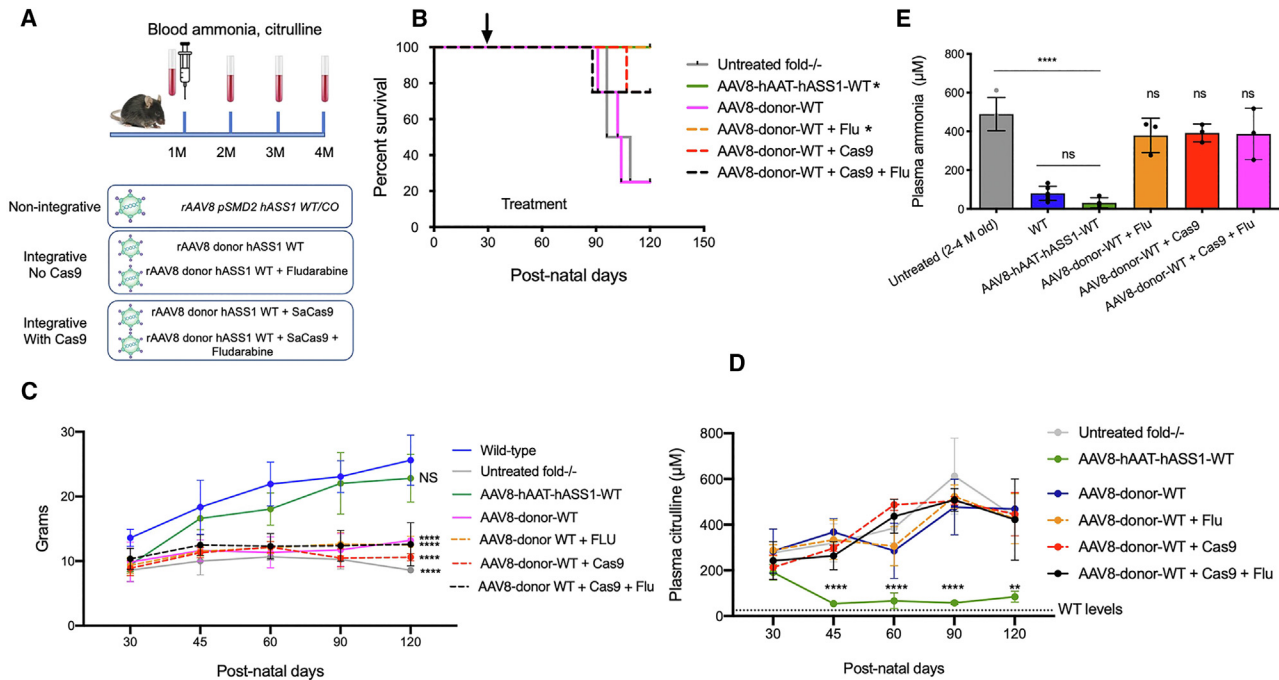


Figure 4. Treatment of juvenile *Ass1* mice with integrative and non-integrative approaches

(A) Scheme of experimental plan. Juvenile *Ass1*^{fold/fold} mice were injected with the different treatments at P30: rAAV8-pSMD2-hASS1 WT (6.0E13 vg/kg); AAV8-donor-hASS1WT (6.0E13 vg/kg); rAAV8-donor-hASS1WT (6.0E13 vg/kg) + fludarabine (3 × 125 mg/kg); rAAV8-donor-hASS1WT (6.0E13 vg/kg) + rAAV8-SaCas9-sg8 (6.0E13 vg/kg); rAAV8-donor-hASS1WT (6.0E13 vg/kg) + rAAV8-SaCas9-sg8 (6.0E13 vg/kg) + fludarabine (3 × 125 mg/kg). Blood was collected at different time points. The experiment was terminated 3 months after the injection (4 months of age), and liver was collected. (B) Kaplan-Meier survival curve. In the curve are represented mice treated with 6.0E13 vg/kg AAV-donor-hASS1 WT and different co-treatments (AAV-Cas9, fludarabine, or both) or with the episomal pSMD2-hAAT-hASS1 WT vector (n = 4 mice per group). The arrow indicates the start of the treatment at P30. Untreated *Ass1*^{fold/fold} animals were used as control. Data were analyzed using log-rank test (Mantel-Cox). (C) Growth curve. In the graph are represented the body weight (mean ± SD) of each experimental group, the untreated group (control) and healthy wild-type animals. Tukey's multiple-comparisons tests, two-way ANOVA: untreated vs. AAV8-hAAT-hASS1-WT, p < 0.0001; AAV8-hAAT-hASS1-WT vs. wild-type, ns; WT vs. all other groups, p < 0.0001; untreated vs. AAV8-donor-WT + Flu, p = 0.031; untreated vs. AAV8-donor-WT + Cas9 + Flu, p = 0.025. (D) Plasma citrulline. In the graph are represented the plasma citrulline levels of mice treated with different AAV-donor-hASS1 WT vector doses and untreated *Ass1*^{fold/fold} group. Data are shown as mean ± SD and were statistically analyzed using two-way ANOVA: treatment, ***p < 0.001; time, ***p < 0.001; interaction, ***p < 0.001. ns, p > 0.05; ****p < 0.0001. (E) Plasma ammonia levels. Plasma ammonia was analyzed at 4 months of age (3 months after the treatment). Data are shown as mean ± SD and were statistically analyzed using one-way ANOVA with Tukey's multiple-comparisons test (***p < 0.001).

lethal mouse model of CTLNI: newborn mice modeling the classical neonatal onset and more severe form of the disease, and juvenile, at 1 month of age, modeling the late-onset, less severe, form of CTLNI. We performed AAV-mediated liver gene replacement therapy and genome targeting and compared their therapeutic efficacy in neonate and juvenile *Ass1*^{fold/fold} mice, a lethal mouse model of the disease.²⁸ We have demonstrated the therapeutic efficacy of both approaches in rescuing mortality and reducing the levels of plasma citrulline, the main marker of disease. The integrative approach proved to be efficacious in neonate mice, while the non-integrative approach was efficacious in juvenile animals.

The neonatal administration of the episomal vector resulted in a minor and statistically nonsignificant amelioration in plasma citrulline values, with no changes in plasma ammonia levels. The failure to correct the phenotype was probably a consequence of the loss of vector DNA, which is associated with hepatocyte proliferation in the growing

liver.^{14–16} Chandler et al.,²⁹ using a similar non-integrative approach, were able to rescue mortality and improve disease markers when *Ass1*^{fold/fold} mice were injected at 7–10 days of life, an age at which the most active phase of hepatocyte proliferation is terminating,³³ resulting, probably, in an overall lower rate of DNA loss compared with P2 treatment and, consequently, higher therapeutic efficacy. Recently, Bazo et al.³⁴ reported the treatment of 3-week-old *Ass1*^{fold/fold} mice with 1.0E14 vg/kg of a non-integrative AAV-Anc80 capsid expressing the human *ASS1* cDNA under the control of a liver-specific promoter, supplemented with ammonia scavengers prior to AAV dosing. This combined treatment resulted in the full mortality rescue, normalization of plasma ammonia and body weight, and improvement in plasma citrulline.³⁴ We observed similar findings to those of Bazo et al. with non-integrative AAV8 transfer in juvenile, P30 mice with a dose of 6.0E13 vg/kg, but without the combined treatment with the nitrogen scavengers agents. These results demonstrate the efficacy of the non-integrative AAV treatment when dosing juvenile-adult

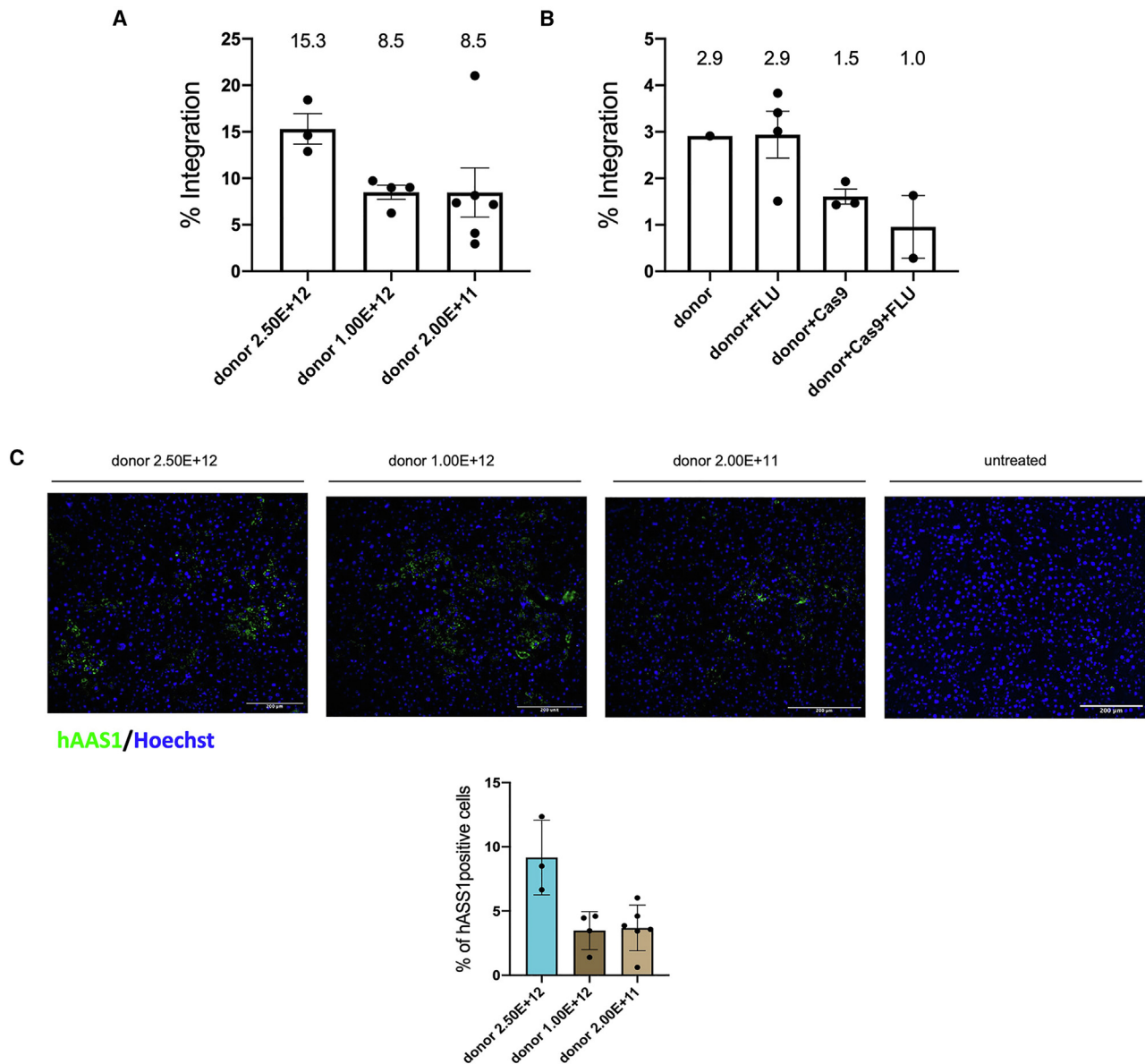


Figure 5. Determination of gene-targeting recombination rate

(A and B) Gene-targeting rate analyzed using ddPCR in genomic liver DNA from mice injected with the gene-targeting strategy at neonatal (A) and juvenile ages (B). Data are expressed as mean \pm SD. (C) FISH analysis of liver sections in mice treated at neonatal age. Representative images are shown in the left panels. The percentage of FISH-positive hepatocytes were quantified, and results are shown in the bar graph. The white bar corresponds to 200 μ m.

mice and provide strong experimental support for its potential translation to the clinic. Considering the partial rescue and improvements in disease parameters reported by Chandler et al.²⁹ in the same mouse model treated with a similar non-integrative approach, we performed our experiments using a higher dose. Nevertheless, further experiments might be necessary to establish the minimal effective dose.

In line with our results, gene-replacement episomal AAV delivery at neonatal age was not sufficient to rescue survival in a severe Aas1

mouse model after a single injection.¹⁷ Survival into adulthood required multiple vector re-administrations,¹⁷ a strategy that in human patients may be limited by the generation of anti-AAV neutralizing antibodies after the first vector administration.^{8,19,35} Different strategies are being investigated to overcome this obstacle, such as the co-administration of immunomodulators, which would allow vector re-administration.³⁶ A potential strategy to obtain long-term therapeutic efficacy is the permanent modification of the genome, a methodology that warrants the transfer of the therapeutic transgene

to daughter cells, allowing a stable therapeutic effect also in proliferating cells.³⁷

A first attempt to modify the genome in urea cycle disease models used the piggyBac transposase in newborn Spf^{Ash} and *in utero* of Ass1^{-/-} mutant mice, models of late-onset OTC deficiency and CTLNI, respectively.³⁸ With this approach the transgene is inserted into “TTAA” sequences, with a preference for transcriptional units.³⁹ Consequently, the translation of this strategy to the clinic is limited by the high risk for insertional mutagenesis, as the integration is not specific. The discovery of site-specific engineered nucleases opened a new era in gene therapy.^{20,40} This strategy was applied by Yang et al.⁴¹ to treat OTC deficiency using a donor vector together with the Cas9 nuclease and a guide RNA to efficiently correct the splice site mutation present in newborn Spf^{Ash} mice. One limitation of this approach resides in the requirement for multiple mutation-specific AAV donor vectors for the corrections of the huge variety of patients’ mutant alleles,^{42,43} making its potential clinical translation more difficult.

Here, we have used a strategy that can be applied to most disease-causing mutations: a SaCas9-mediated genome targeting approach that inserts a copy of the full ASS1 cDNA into the albumin ORF, which remains under the transcriptional control of the robust albumin gene promoter.^{25–27} The treatment of neonatal Ass1^{fold/fold} mice with the gene targeting approach resulted in the full rescue of disease mortality with all AAV-donor doses tested. Analysis of plasma citrulline levels showed a significant reduction of this key disease marker in all groups, almost reaching WT values in the group treated with the higher AAV dose. However, we observed a minor, statistically nonsignificant reduction in plasma ammonia levels, suggesting that the GeneRide approach requires further improvements before it can be successfully implemented in a clinical setting.

The required rates of correction levels vary from disease to disease both in patients and in animal models. Hemophilia B is a favorable disease for gene therapy treatment, as a low correction rate (from 1% to 5%) is enough to restore a minimal threshold of factor IX levels and convert the disease into a moderate form.⁴⁴ In Crigler-Najjar syndrome type I patients, a minimum of 5% of UGT1A1 activity is required to obtain a partial reduction in plasma bilirubin reaching safer levels.⁴⁵ In some urea cycle disorders, higher therapeutic levels are probably required, as heterozygous OTCD female carriers may present symptoms of the disease even if in milder and later forms.⁴⁶ In fact, Spf^{Ash} mice, a strain with residual 6%–8% of OTC activity, were treated with two gene-targeting approaches in which about 10% of corrected hepatocytes were enough to achieve a rescue of the disease.^{41,47}

Thus, CTLNI, like OTC deficiency and other urea cycle disorders, may require a higher protein level to achieve the same results. With the GeneRide strategy the therapeutic protein is overexpressed by the targeted hepatocytes and it can reach higher protein levels than those present in a healthy liver.^{26,27} Consequently, the amelioration

or normalization of the phenotype may require a lower proportion of targeted cells. In fact, the Crigler-Najjar type I mouse model can be completely rescued from lethality (albeit without normalization of plasma bilirubin levels) with GeneRide targeting rates in the range of 0.04%, without the use of nucleases.^{23,26} When we applied the SaCas9 nuclease in combination with the GeneRide strategy, we increased the rate of targeting up to 3.6%, resulting in the complete normalization of all parameters.²⁶ In a hemophilia B mouse model, 0.5% of recombinant hepatocytes resulted in 5%–20% of circulating FIX levels,²⁷ while the use of nucleases increased the targeting rate to 4%, which resulted in up to 140%–200% of circulating FIX levels, completely correcting the bleeding phenotype.²⁵ Our data in the newborn Ass1^{fold/fold} mice showed that 9%–15% of targeted hepatocytes after neonatal delivery were sufficient to fully rescue mortality and significantly ameliorate the disease markers, as determined using FISH and ddPCR, with a dose-response pattern. We separately treated mice with two AAV vectors containing WT or codon-optimized AAS1 cDNAs. Surprisingly, the codon-optimized vector exhibited lower activity than the WT, contrary to our expectations. The scarce activity may be attributed to the optimization of codon use for human cells, which resulted in a different effect when used *in vivo*.

Despite the promising results obtained in neonatal mice, the approach was less effective when applied to juvenile animals. It is well known that the gene-targeting rate is less efficient in non-duplicating cells, which is associated with a decreased activity of the HDR DNA repair mechanism and the preferential activation of the nonhomologous end joining (NHEJ) DNA repair mechanism in the adult liver,⁴⁸ although we had observed that the majority of AAV-HR events occurred in non-proliferating hepatocytes in juvenile mouse livers.³² Nonetheless, the rate of gene targeting achieved with the GeneRide approach in juvenile Ass1^{fold/fold} mice, with or without the use of nucleases and fludarabine, was not sufficient to rescue the phenotype. It presented a lower targeting rate, reaching up to 3% as determined using ddPCR analysis, in the groups without nuclease. Similarly to our results, gene correction in Spf^{Ash} mice or GeneRide in adult hemophilia B animals was not effective in adult animals.^{25,41} The higher targeting rate observed in the neonatal group is in line with the proliferative status of the liver and the more active HDR DNA repair mechanism in duplicating cells.⁴⁹ These results suggest that a minimum of 8% of targeted hepatocytes by the GeneRide approach may be necessary for mortality rescue and partial correction of the phenotype in Ass1^{fold/fold} mice, while lower levels are not sufficient to rescue mortality.

One important concern of genome targeting approaches with the use of engineered nucleases regards the potential off-target activity and risk for tumorigenesis.⁵⁰ The specificity and the absence of off-target nuclease activity of the approach used here and in previous studies were analyzed by amplifying and sequencing on- and off-target predicted amplicons.²⁶ Further analysis of other safety parameters detected no changes in albumin levels, immune response, liver abnormalities, or tumorigenesis, supporting the overall safety of the approach.²⁶

To summarize, we presented here results supporting two potential therapies for “classical” neonatal and late-onset forms of CTLN1. We have shown that the gene targeting approach, exploiting the use of the CRISPR/SaCas9 platform, is the most effective one for its potential application in neonatal settings. In contrast, for the late-onset form of CTLN1, presenting symptoms at juvenile/adult age, the AAV-mediated liver-specific non-integrative gene therapy is the most effective one, resulting in the complete and long-term normalization of the main disease markers and thus providing strong support for its potential translation to the clinic.

MATERIALS AND METHODS

ASS1^{fold/fold} mice

CTLN1 mice, strain B6Ei.PAss1<fold>/Grsr], were purchased from The Jackson Laboratory (stock number 006449). The colony was expanded and maintained in the ICGEB experimental facility. Animals were housed and handled according to institutional guidelines, and experimental procedures approved by International Centre for Genetic Engineering and Biotechnology (ICGEB) review board, following European Union (EU) Directive 2010/63/EU for animal experimentation, with the previous approval of the Italian Ministry of Health (authorization number 123/2019-PR). All animal experiments conform to all relevant regulatory standards. Mice were maintained in the ICGEB animal house unit in a temperature-controlled environment with 12 h light-dark cycles and received a standard chow diet and water *ad libitum*. Mixed groups of male and female mutant animals were used for the experiments.

rAAV vectors

Human WT and four codon-optimized versions of the human ASS1 cDNA were inserted into the pGEM cloning vector. Codon-optimized cDNA versions were generated with different optimization algorithms from online platforms (Genescript, IDT, JCat,⁵¹ GeneArt).

hASS1 WT and codon-optimized cDNA number 1 were cloned into the pSMD2 vector containing the alpha-1-antitrypsin (hAAT) promoter and the apolipoprotein E (ApoE) enhancer,²² in a modified version of the AAV-donor vector as described previously.²⁶

The recombinant AAV vectors pseudo-serotyped with the AAV8 capsid proteins were prepared by AAV Vector Unit at ICGEB Trieste and Génethon Institute in Paris. hASS1 WT/CO cDNAs were inserted into the pAB288 donor vector as described previously.^{25,26}

Cell transfection

HUH-7 liver-derived cells were transfected with pGEM vectors encoding the WT and four different codon-optimized hASS1 cDNAs. eGFP plasmid was co-transfected as transfection control. The Lipofectamine 2000 transfection reagent used was purchased from Invitrogen and used following the manufacturer's protocol.

rAAV treatment of neonate and juvenile ASS1^{fold/fold} mice

Mice were injected intravenously (i.v.) through retro-orbital injection at P2 or P30. Mice at P2 were treated with 2.0E+11 of AAV-pSMD2-

a1AAT-hASS1-WT/CO and 2.0E+11, 1.00E+12, and 2.5E+12 of AAV-donor-hASS1-WT/CO and 2,0E11 of AAV-SaCas9 per mouse.

Mice at P30 were anesthetized and treated with a retro-orbital injection with 6.0E+13 vg/kg AAV-pSMD2-hAAT-hASS1 WT and AAV-donor-hASS1 WT and 6,0E12 vg/kg AAV-SaCas9. Fludarabine (9-beta-D-arabinofuranosyl-2-fluoroadenine 5) was injected through intraperitoneal (i.p.) injection at 125 mg/kg for three days (P30–P32).

Blood collection

Mice were previously anesthetized and blood was collected through facial vein bleeding in anesthetized animals, as described previously (De Caneva, JCI Insight, 2019). The blood was centrifuged at $3,000 \times g$ for 15 min at 4°C, and the plasma was stored at –80°C.

Citrulline analysis

Plasma citrulline was evaluated in the Biotechnology Transfer Unit at the ICGEB in Trieste. L-citrulline was purchased from Merck-Sigma-Aldrich, and the isotopically labeled internal standard L-citrulline-4,4,5,5-d4 was purchased from Cambridge Biolabs. The quantitative experiments were done using as internal standard the isotopically labeled L-Citrulline-4,4,5,5-d4 in 10 μM concentration both for the calibration curve and samples. A typical calibration curve ranged from 0 to 800 μM with excellent linearity ($R^2 > 0.99$). A Bruker (Bremen, Germany) amaZonSL bench-top ion trap mass spectrometer, equipped with an electrospray source, was used for this study. The source was operated in positive ion mode with a needle potential of 4,500 V and nitrogen nebulizer at 44 psi with dry gas 8 L/min at 200°C. The chromatographic separations for quantitative experiments were performed using a series 1260 Agilent Technologies (Waldbronn, Germany) high-performance liquid chromatograph (HPLC) with autosampler controlled from the Bruker HyStar data system. An Agilent ZORBAX HILIC Plus HPLC column, 2.1 × 50 mm at 30°C, was used. The column flow rate was 0.5 mL/min, and elution was performed using 3 min wash time after 5 μL injection and a 10 min gradient from 95% acetonitrile/5% water with 0.1% formic acid to water with 0.1% formic acid. The retention time of citrulline and internal standard in these conditions was 7.8 min. The tandem mass spectrometry (MS/MS) transitions used for the quantitative experiments (multiple reaction monitoring [MRM]) were m/z 176.2–159.1 (citrulline) and 180.2–163.1 (L-citrulline-4,4,5,5-d4). The acquired data were processed using the Bruker Compass Data Analysis 4.2 software and quantified using the Bruker Quant Analysis 2.2 software.

Ammonia analysis

Ammonia was analyzed spectrophotometrically with the Ammonia Assay Kit from Sigma-Aldrich (AA0100) following the indication provided. Plasma (10 μL) was diluted in 10 μL water to reach a final volume of 20 μL. To each sample, 200 μL Ammonia Assay Reagent was added. After 5 min of incubation at room temperature, absorbance was read at 340 nm. Afterward, 2 μL L-glutamate solution was added to each sample and incubated for 5 min, and the absorbance was

re-measured at 340 nm. Ammonia levels were calculated in milligrams of NH₃ per milliliter, as described in the manufacturer's instructions.

ddPCR

On-target integration rate was analyzed using ddPCR using a previously described protocol.^{25,32} Genomic DNA was extracted from frozen liver powder using the SV Genomic DNA Purification System by Promega following the manufacturer's instructions. The amplification of the 1.6 kb non-targeted region of endogenous mouse albumin was performed using a forward 5'-CTGCTGTGCACCAGTTGATGTT-3' and reverse 5'-TGCTTTCTGGGTGTAGCGAACT-3' primer, combined with a HEX-labeled probe 5'-TCTGGTGCTGAGGACACGTAGCCCAGT-3'. The on-target HR (1.4 kb amplicon) was amplified using a forward 5'-GGGCAAGGCAACGTCATGG-3' and reverse 5'-CCAGGGTCTCTTCCACGTC-3' primer, combined with a FAM-labeled probe (5'-GCCCAAGGCTAC AGCGGAGC-3').

FISH

Fixed liver cryosections were permeabilized with PBS 1×, 0.1% Tween and 0.5% Triton for 20 min. *hASS1* mRNA was detected in liver sections using the HRC RNA-FISH Technology kit purchased from Molecular Instruments, using the manufacturer's protocol. Briefly, 100 μL hybridization buffer was added to the liver section and incubated in a humidified chamber for 10 min at 37°C. Next, 0.4 pmol *hASS1*-specific probes and 100 μL hybridization buffer were added to the liver section and left incubating overnight in a humidified chamber at 37°C. The next day, probe wash buffer was added to slides and left at 37°C for 10 min. Following probe washes at 37°C with 75% of probe wash buffer and 25% 5× SSCT for 15 min, 50% of probe wash buffer and 50% 5× SSCT for 15 min, 25% of probe wash buffer and 75% 5× SSCT for 15 min, 100% 5× SSCT for 15 min. The last wash used 5× SSCT for 5 min at room temperature. To pre-amplify the probe, 100 μL amplification buffer was added to slides and left incubating in a humidified chamber at 37°C for 30 min. In the meantime, 6 pmol of hairpin h1 and 6 pmol of hairpin h2 were activated at 95°C for 90 s and left to cool down to room temperature for 30 min in dark. Hairpins were mixed with 100 μL of amplification buffer, added to the sample and incubated overnight in a humidified chamber at room temperature. 5× SSCT was used to remove excess hairpins for 2 × 30 min and 1 × 5 min. Nuclei were stained with Hoechst for 5 min and washed three times with PBS 1×. Fluorescent images were taken using a Nikon fluorescent microscope.

mRNA expression analysis

RNA was extracted by homogenizing liver powder in NucleoZOL solution (Takara Bio) following the manufacturer's protocol. Total RNA (1 μg) was reverse-transcribed using M-MLV reverse transcriptase (Invitrogen, Carlsbad, CA) following the supplier's protocol and as previously described.²⁵

Chimeric *hASS1-Alb* mRNA expression levels were measured with a qRT-PCR using *hASS1* WT (forward 5'-AGGAGCTGGTGAGCATGAAC-3' and reverse 5'-TGAGTCCTGAGTCTTCATGTCTT-3') and codon-optimized specific primers (forward 5'-GGAGCTGGTC

TCTATGAACG-3' and reverse 5'-TGAGTCCTGAGTCTTCATGTCTT-3').

Viral genome copy number analysis

Viral genome copy number was analyzed by extracting liver DNA using SV Genomic DNA Purification System by Promega following the manufacturer's instructions. Viral DNA was analyzed as previously described.²⁵ Episomal rAAV-pSMD2 vector was analyzed using a forward 5'-GCCACTAAGGATTCTGCAGT-3' and reverse 5'-CTGCACTTACCGAAAGGAGT-3' primer, the donor vector using a forward 5'-ACTTCTGTCTCTGTGCTGC-3' and reverse 5'-TGATTAACCCGCCATGCTAC-3' primer, and the AAV-Cas9 DNA using a forward 5'-AAGGATCACCCAGCCTCTGC-3' and reverse 5'-CCTGCTGAAGACACTCTTGCCA-3' primer.

Primer efficiency analysis

The hybrid *hASS1-Alb* WT or CO mRNAs in treated mice and endogenous mouse *Ass1* mRNA in WT mice were amplified using PCR and quantified on nanodrop. After, 1:10 serial dilutions were made using the two amplicons, starting from 0.2 ng, and analyzed using qPCR.

The Cq mean values and the template quantity of both amplicons were plotted in a graph and compared.

Western blot analysis

Proteins were obtained from homogenized liver powder in a lysis buffer as previously described.²⁵ Primary antibody anti-ASS1 was purchased from Invitrogen (catalog #OTI12G1) and the anti-Hsp70 from Enzo (catalog #ADI-SPA-815-D) and were diluted at 1:3,000 and 1:8,000, respectively. The anti-eGFP antibody was purchased from Santa Cruz (catalog #sc8334) and diluted 1:3,000 before use.

Statistical analysis

Statistical analyses were performed using GraphPad Prism 8.2.1. Student's t test and one-way or two-way ANOVA were used, and a p value <0.05 was considered to indicate statistical significance. Data in the graphs are expressed as mean ± SD.

DATA AND CODE AVAILABILITY

The materials presented here are available for distribution after the execution of a material transfer agreement (MTA) with the ICGEB.

SUPPLEMENTAL INFORMATION

Supplemental information can be found online at <https://doi.org/10.1016/j.omtm.2023.08.022>.

ACKNOWLEDGMENTS

This work was supported by an AFM-Téléthon grant (ID21826) to A.F.M. and by ICGEB intramural funds. We would like to thank the staff of the ICGEB adeno-associated vector unit (AVU) and the bioexperimentation facilities for technical support. We thank Viktoriya Sidarovich and Pamela Gatto of HTS and Validation Core Facility, Dep. CIBIO, University of Trento for performing ddPCR experiments.

AUTHOR CONTRIBUTIONS

Conceptualization, M.L. and A.F.M.; Data Collection, Analysis, and Interpretation, M.L., A.I., C.G., A.V., L.M., F.C., G.R., L.Z., and A.F.M.; Manuscript Preparation, M.L. and A.F.M.; Critical Appraisal and Manuscript Review and Editing: M.L., A.I., C.G., A.V., L.M., F.C., G.R., L.Z., and A.F.M.

DECLARATION OF INTERESTS

A.F.M. is an inventor on patents describing liver gene transfer approaches for metabolic diseases and/or treatment of hyperbilirubinemia.

REFERENCES

- Beaudet, A.L., O'Brien, W.E., Bock, H.G., Freytag, S.O., and Su, T.-S. (1986). The Human Argininosuccinate Synthetase Locus and Citrullinemia. *Adv. Hum. Genet.* 15, 161–196. 291–292.
- Woo, H.I., Park, H.-D., and Lee, Y.-W. (2014). Molecular genetics of citrullinemia types I and II. *Clin. Chim. Acta* 431, 1–8.
- Häberle, J., Burlina, A., Chakrapani, A., Dixon, M., Karall, D., Lindner, M., Mandel, H., Martinelli, D., Pintos-Morell, G., et al. (2019). Suggested guidelines for the diagnosis and management of urea cycle disorders: First revision. *J. Inher. Metab. Dis.* 42, 1192–1230.
- Vara, R., Dhawan, A., Deheragoda, M., Grünewald, S., Pierre, G., Heaton, N.D., Vilca-Melendez, H., and Hadžić, N. (2018). Liver transplantation for neonatal-onset citrullinemia. *Pediatr. Transplant.* 22, e13191.
- Liu, Y., Luo, Y., Xia, L., Qiu, B., Zhou, T., Feng, M., Wang, C., Xue, F., Chen, X., Han, L., et al. (2021). Outcome of Liver Transplantation for Neonatal-onset Citrullinemia Type I. *Transplantation* 105, 569–576.
- Pasi, K.J., Rangarajan, S., Mitchell, N., Lester, W., Symington, E., Madan, B., Laffan, M., Russell, C.B., Li, M., Pierce, G.F., and Wong, W.Y. (2020). Multiyear Follow-up of AAV5-hFVIII-SQ Gene Therapy for Hemophilia A. *N. Engl. J. Med.* 382, 29–40.
- Nathwani, A.C., Tuddenham, E.G.D., Rangarajan, S., Rosales, C., McIntosh, J., Linch, D.C., Chowdhary, P., Riddell, A., Pie, A.J., Harrington, C., et al. (2011). Adenovirus-associated virus vector-mediated gene transfer in hemophilia B. *N. Engl. J. Med.* 365, 2357–2365.
- Nathwani, A.C., Reiss, U.M., Tuddenham, E.G.D., Rosales, C., Chowdhary, P., McIntosh, J., Della Peruta, M., Lheriteau, E., Patel, N., Raj, D., et al. (2014). Long-term safety and efficacy of factor IX gene therapy in hemophilia B. *N. Engl. J. Med.* 371, 1994–2004.
- Rangarajan, S., Walsh, L., Lester, W., Perry, D., Madan, B., Laffan, M., Yu, H., Vettermann, C., Pierce, G.F., Wong, W.Y., and Pasi, K.J. (2017). AAV5-Factor VIII Gene Transfer in Severe Hemophilia A. *N. Engl. J. Med.* 377, 2519–2530.
- George, L.A., Sullivan, S.K., Giermasz, A., Rasko, J.E.J., Samelson-Jones, B.J., Ducore, J., Cuker, A., Sullivan, L.M., Majumdar, S., Teitel, J., et al. (2017). Hemophilia B Gene Therapy with a High-Specific-Activity Factor IX Variant. *N. Engl. J. Med.* 377, 2215–2227.
- Wang, L., Zoppè, M., Hackeng, T.M., Griffin, J.H., Lee, K.F., and Verma, I.M. (1997). A factor IX-deficient mouse model for hemophilia B gene therapy. *Proc. Natl. Acad. Sci. USA* 94, 11563–11566.
- Wang, L., Nichols, T.C., Read, M.S., Bellinger, D.A., and Verma, I.M. (2000). Sustained Expression of Therapeutic Level of Factor IX in Hemophilia B Dogs by AAV-Mediated Gene Therapy in Liver. *Mol. Ther.* 1, 154–158.
- Mount, J.D., Herzog, R.W., Tillson, D.M., Goodman, S.A., Robinson, N., McClelland, M.L., Bellinger, D., Nichols, T.C., Arruda, V.R., Lothrop, C.D., and High, K.A. (2002). Sustained phenotypic correction of hemophilia B dogs with a factor IX null mutation by liver-directed gene therapy. *Blood* 99, 2670–2676.
- Bortolussi, G., Zentilin, L., Vaníkova, J., Bockor, L., Bellarosa, C., Mancarella, A., Vianello, E., Tiribelli, C., Giacca, M., Vitek, L., and Muro, A.F. (2014). Life-long correction of hyperbilirubinemia with a neonatal liver-specific AAV-mediated gene transfer in a lethal mouse model of Crigler-Najjar Syndrome. *Hum. Gene Ther.* 25, 844–855.
- Wang, L., Wang, H., Bell, P., McMenamin, D., and Wilson, J.M. (2012). Hepatic gene transfer in neonatal mice by adeno-associated virus serotype 8 vector. *Hum. Gene Ther.* 23, 533–539.
- Cunningham, S.C., Dane, A.P., Spinoulas, A., Alexander, I.E., and Alexander, I.E. (2008). Gene delivery to the juvenile mouse liver using AAV2/8 vectors. *Mol. Ther.* 16, 1081–1088.
- Kok, C.Y., Cunningham, S.C., Carpenter, K.H., Dane, A.P., Siew, S.M., Logan, G.J., Kuchel, P.W., and Alexander, I.E. (2013). Adeno-associated virus-mediated rescue of neonatal lethality in argininosuccinate synthetase-deficient mice. *Mol. Ther.* 21, 1823–1831.
- Patejunas, G., Bradley, A., Beaudet, A.L., and O'Brien, W.E. (1994). Generation of a mouse model for citrullinemia by targeted disruption of the argininosuccinate synthetase gene. *Somat. Cell Mol. Genet.* 20, 55–60.
- George, L.A., Ragni, M.V., Rasko, J.E.J., Raffini, L.J., Samelson-Jones, B.J., Ozelo, M., Hazbon, M., Runowski, A.R., Wellman, J.A., Wachtel, K., et al. (2020). Long-Term Follow-Up of the First in Human Intravascular Delivery of AAV for Gene Transfer: AAV2-hFIX16 for Severe Hemophilia B. *Mol. Ther.* 28, 2073–2082.
- Carroll, D. (2014). Genome engineering with targetable nucleases. *Annu. Rev. Biochem.* 83, 409–439.
- Trevisan, M., Masi, G., and Palù, G. (2020). Genome editing technologies to treat rare liver diseases. *Transl. Gastroenterol. Hepatol.* 5, 23.
- Ronzitti, G., Bortolussi, G., van Dijk, R., Collaud, F., Charles, S., Leborgne, C., Vidal, P., Martin, S., Gjata, B., Sola, M.S., et al. (2016). A translationally optimized AAV-UGT1A1 vector drives safe and long-lasting correction of Crigler-Najjar syndrome. *Mol. Ther. Methods Clin. Dev.* 3, 16049.
- Porro, F., Bortolussi, G., Barzel, A., De Caneva, A., Iaconcig, A., Vodret, S., Zentilin, L., Kay, M.A., and Muro, A.F. (2017). Promoterless gene targeting without nucleases rescues lethality of a Crigler-Najjar syndrome mouse model. *EMBO Mol. Med.* 9, 1346–1355.
- Nygaard, S., Barzel, A., Haft, A., Major, A., Finegold, M., Kay, M.A., and Grompe, M. (2016). A universal system to select gene-modified hepatocytes in vivo. *Sci. Transl. Med.* 8, 342ra79.
- Lisjak, M., De Caneva, A., Marais, T., Barbon, E., Biferi, M.G., Porro, F., Barzel, A., Zentilin, L., Kay, M.A., Mingozzi, F., and Muro, A.F. (2022). Promoterless Gene Targeting Approach Combined to CRISPR/Cas9 Efficiently Corrects Hemophilia B Phenotype in Neonatal Mice. *Front. Genome Ed.* 4, 785698.
- De Caneva, A., Porro, F., Bortolussi, G., Sola, R., Lisjak, M., Barzel, A., Giacca, M., Kay, M.A., Vlahoviček, K., Zentilin, L., and Muro, A.F. (2019). Coupling AAV-mediated promoterless gene targeting to SaCas9 nuclease to efficiently correct liver metabolic diseases. *JCI Insight* 5, e128863.
- Barzel, A., Paulk, N.K., Shi, Y., Huang, Y., Chu, K., Zhang, F., Valdmanis, P.N., Spector, L.P., Porteus, M.H., Gaensler, K.M., and Kay, M.A. (2015). Promoterless gene targeting without nucleases ameliorates haemophilia B in mice. *Nature* 517, 360–364.
- Perez, C.J., Jaubert, J., Guénet, J.L., Barnhart, K.F., Ross-Inta, C.M., Quintanilla, V.C., Aubin, I., Brandon, J.L., Otto, N.W., DiGiovanni, J., et al. (2010). Two hypomorphic alleles of mouse *Ass1* as a new animal model of citrullinemia type I and other hyperammonemic syndromes. *Am. J. Pathol.* 177, 1958–1968.
- Chandler, R.J., Tarasenko, T.N., Cusmano-Ozog, K., Sun, Q., Sutton, V.R., Venditti, C.P., and McGuire, P.J. (2013). Liver-directed adeno-associated virus serotype 8 gene transfer rescues a lethal murine model of citrullinemia type I. *Gene Ther.* 20, 1188–1191.
- Porro, F., Rosato-Siri, M., Leone, E., Costessi, L., Iaconcig, A., Tongiorgi, E., and Muro, A.F. (2010). beta-adducin (Add2) KO mice show synaptic plasticity, motor coordination and behavioral deficits accompanied by changes in the expression and phosphorylation levels of the alpha- and gamma-adducin subunits. *Genes Brain Behav.* 9, 84–96.
- Liu, Z., Dong, L., Wang, L., Wang, X., Cheng, K., Luo, Z., Weng, W., Qian, L., and Liu, J. (2017). Systematic comparison of 2A peptides for cloning multi-genes in a polycistronic vector. *Sci. Rep.* 7, 17926.

32. Tsuji, S., Stephens, C.J., Bortolussi, G., Zhang, F., Baj, G., Jang, H., de Alencastro, G., Muro, A.F., Pekrun, K., and Kay, M.A. (2022). Fludarabine increases nuclease-free AAV- and CRISPR/Cas9-mediated homologous recombination in mice. *Nat. Biotechnol.* *40*, 1285–1294.
33. Fausto, N., Laird, A.D., and Webber, E.M. (1995). Liver regeneration. 2. Role of growth factors and cytokines in hepatic regeneration. *FASEB J.* *9*, 1527–1536.
34. Bazo, A., Lantero, A., Mauleón, I., Neri, L., Poms, M., Häberle, J., Ricobaraza, A., Bénichou, B., Combal, J.-P., Gonzalez-Aseguinolaza, G., and Aldabe, R. (2022). Gene Therapy in Combination with Nitrogen Scavenger Pretreatment Corrects Biochemical and Behavioral Abnormalities of Infant Citrullinemia Type 1 Mice. *Int. J. Mol. Sci.* *23*, 14940.
35. Mingozzi, F., and High, K.A. (2017). Overcoming the Host Immune Response to Adeno-Associated Virus Gene Delivery Vectors: The Race Between Clearance, Tolerance, Neutralization, and Escape. *Annu. Rev. Virol.* *4*, 511–534.
36. Meliani, A., Boisgerault, F., Hardet, R., Marmier, S., Collaud, F., Ronzitti, G., Leborgne, C., Costa Verdera, H., Simon Sola, M., Charles, S., et al. (2018). Antigen-selective modulation of AAV immunogenicity with tolerogenic rapamycin nanoparticles enables successful vector re-administration. *Nat. Commun.* *9*, 4098.
37. Kay, M.A. (2011). State-of-the-art gene-based therapies: the road ahead. *Nat. Rev. Genet.* *12*, 316–328.
38. Cunningham, S.C., Siew, S.M., Hallwirth, C.V., Bolitho, C., Sasaki, N., Garg, G., Michael, I.P., Hetherington, N.A., Carpenter, K., de Alencastro, G., et al. (2015). Modeling correction of severe urea cycle defects in the growing murine liver using a hybrid recombinant adeno-associated virus/piggyBac transposase gene delivery system. *Hepatology* *62*, 417–428.
39. Ding, S., Wu, X., Li, G., Han, M., Zhuang, Y., and Xu, T. (2005). Efficient Transposition of the piggyBac (PB) Transposon in Mammalian Cells and Mice. *Cell* *122*, 473–483.
40. Doudna, J.A., and Charpentier, E. (2014). The new frontier of genome engineering with CRISPR-Cas9. *Science* *346*, 1258096.
41. Yang, Y., Wang, L., Bell, P., McMenamin, D., He, Z., White, J., Yu, H., Xu, C., Morizono, H., Musunuru, K., et al. (2016). A dual AAV system enables the Cas9-mediated correction of a metabolic liver disease in newborn mice. *Nat. Biotechnol.* *34*, 334–338.
42. Choi, J.-H., Lee, B.H., Kim, J.H., Kim, G.-H., Kim, Y.-M., Cho, J., Cheon, C.-K., Ko, J.M., Lee, J.H., and Yoo, H.-W. (2015). Clinical outcomes and the mutation spectrum of the OTC gene in patients with ornithine transcarbamylase deficiency. *J. Hum. Genet.* *60*, 501–507.
43. Caldovic, L., Abdikarim, I., Narain, S., Tuchman, M., and Morizono, H. (2015). Genotype-Phenotype Correlations in Ornithine Transcarbamylase Deficiency: A Mutation Update. *J. Genet. Genom.* *42*, 181–194.
44. Mannucci, P.M., and Tuddenham, E.G. (2001). The Hemophilias — From Royal Genes to Gene Therapy. *N. Engl. J. Med.* *344*, 1773–1779.
45. Fox, I.J., Chowdhury, J.R., Kaufman, S.S., Goertzen, T.C., Chowdhury, N.R., Warkentin, P.L., Dorko, K., Sauter, B.V., and Strom, S.C. (1998). Treatment of the Crigler-Najjar syndrome type I with hepatocyte transplantation. *N. Engl. J. Med.* *338*, 1422–1426.
46. Batshaw, M.L., Msall, M., Beaudet, A.L., and Trojak, J. (1986). Risk of serious illness in heterozygotes for ornithine transcarbamylase deficiency. *J. Pediatr.* *108*, 236–241.
47. Wang, L., Lu, C., Yang, S., Sun, P., Wang, Y., Guan, Y., Liu, S., Cheng, D., Meng, H., Wang, Q., et al. (2020). A mutation-independent CRISPR-Cas9-mediated gene targeting approach to treat a murine model of ornithine transcarbamylase deficiency. *Sci. Adv.* *6*, eabc6686.
48. Xue, C., and Greene, E.C. (2021). DNA Repair Pathway Choices in CRISPR-Cas9-Mediated Genome Editing. *Trends Genet.* *37*, 639–656.
49. Symington, L.S., and Gautier, J. (2011). Double-Strand Break End Resection and Repair Pathway Choice. *Annu. Rev. Genet.* *45*, 247–271.
50. Fu, Y., Foden, J.A., Khayter, C., Maeder, M.L., Reyon, D., Joung, J.K., and Sander, J.D. (2013). High-frequency off-target mutagenesis induced by CRISPR-Cas nucleases in human cells. *Nat. Biotechnol.* *31*, 822–826.
51. Grote, A., Hiller, K., Scheer, M., Münch, R., Nörtemann, B., Hempel, D.C., and Jahn, D. (2005). JCat: a novel tool to adapt codon usage of a target gene to its potential expression host. *Nucleic Acids Res.* *33*, W526–W531.